Visakhapatnam Chapter

Proceedings of Indian Geotechnical Conference 2020
December 17-19, 2020, Andhra University, Visakhapatnam

Effect of EPS Geofoam on Lateral Earth Pressure Reduction – A Numerical Study

Neeraj Kumar Burugupelly[1] and Satyanarayana Murty Dasaka[2]

[1]Graduate Student, Department of Civil Engineering, IIT Bombay, Mumbai, India.
[2] Professor, Department of Civil Engineering, IIT Bombay, Mumbai, India
dasaka@civil.iitb.ac.in

Abstract: Expanded Polystyrene (EPS) geofoam can be used to reduce the lateral thrust on the rigid retaining wall structures. This technique involves providing a layer of geofoam blocks of required dimensions and stiffness between the wall face and the backfill soil. In the present study, finite element numerical program, PLAXIS 2D, was used to carry out parametric study to investigate the influence of height of retaining wall, density and thickness of geofoam on the extent of lateral thrust reduction. Mohr-Coulomb constitutive law was used to model cohesionless backfill material and EPS compressible inclusion. The required material parameters were obtained from the laboratory testing. Modified direct shear tests were carried out to measure shear strength and interface properties of geofoam-concrete, geofoam-sand and concrete-sand interfaces. The model results were validated using the results of small-scale physical model tests from published literature. Analysis was carried out considering different combinations consisting of 5 different wall heights, 4 different densities and 5 different thicknesses of EPS geofoam. The total lateral earth force on the wall and isolation efficiency were computed to evaluate the influence of these parameters on earth pressure reduction. The results clearly show that use of EPS geofoam significantly reduces lateral thrust on the retaining walls, and can substantially bring cost saving in the project.

Keywords: Compressible Inclusion, Modified Direct Shear Test, EPS Geofoam, Parametric Analysis.

1. Introduction

In most cases of rigid retaining wall systems, wall movements are highly restricted such as basement walls, bridge abutments, box culverts, etc. fall under this category. In designing these walls at-rest lateral earth pressures are generally considered. This results in greater magnitudes of lateral earth pressures, resulting in larger cross-sectional dimensions of the wall, making it highly uneconomical and requires larger volumes of materials.

Horvath (1997) concluded that by placing lightweight compressible material like foam behind the retaining wall, these lateral earth pressures can be reduced significantly. This technique of using compressible inclusion involves placing of a highly compressible material between the soil backfill and retaining wall. By placing the compressible inclusion, room for the lateral movement of soil is created so that, the soil can change its state from at-rest condition to active condition. Expanded Polystyrene (EPS) geofoam material is most widely used material for compressible inclusion purpose because of its wide availability, absence of release of gases such as

Formaldehyde post its production (Stark et al. 2004) and it can be manufactured with required stiffness without compromising on its low unit weight. Several researchers (Karpurapu and Bathurst 1992; Zarnani and Bathurst 2008; Athanasopoulus et al. 2012; and Abdelsalam and Azzam 2015) carried out numerical parametric studies to understand the behavior of rigid retaining walls with EPS geofoam compressible inclusions. In the current study PLAXIS 2D software was used to carry out numerical parametric analysis, to quantify the effect of various parameters like height of retaining wall, density and thickness of geofoam inclusion on the extent of lateral thrust reduction on rigid retaining wall.

The work was carried out in two stages. First stage involves performing set of laboratory experiments to characterize the locally available geofoam material. In the second stage, numerical simulations were carried out to understand the influence of the various parameters on lateral earth pressure reduction.

2. Material Testing and Characterization

This section details the experimental work carried out to obtain the material and interface parameters required for the constitutive modelling and calibration of numerical model. The experimental program includes performing 9 static compression tests on EPS geofoam cubes to obtain its compressive strength parameters, set of 3 UU Triaxial tests on cylindrical EPS geofoam samples to determine its shear strength properties and 9 interface shear tests to determine the interface properties of Geofoam–Sand, Geofoam–Concrete and Sand–Geofoam interfaces.

2.1 Static Compression Tests

Static compression tests were performed to evaluate the initial Young's modulus (E), compressive strength (σ_c), yield strength (σ_y) and elastic limit of EPS geofoam. The slope of tangent to the initial linear region of stress strain curve is the initial Young's modulus (Stark et al. 2004). Yield strength is the stress corresponding to point obtained by intersecting initial tangent and back tangent to linear portion of curve at higher strains. Testing was carried in accordance with ASTM D6817M-17 50 x 50 x 50 mm size cubic samples of EPS geofoam of density 20 kg/m^3 were acquired from INSUPAC Industries LTD, Mumbai, for the testing purpose. A strain rate of 10%/min was adopted. As per ASTM D7180-05, stress level corresponding to 10% axial strain was taken as compressive strength of the EPS geofoam.

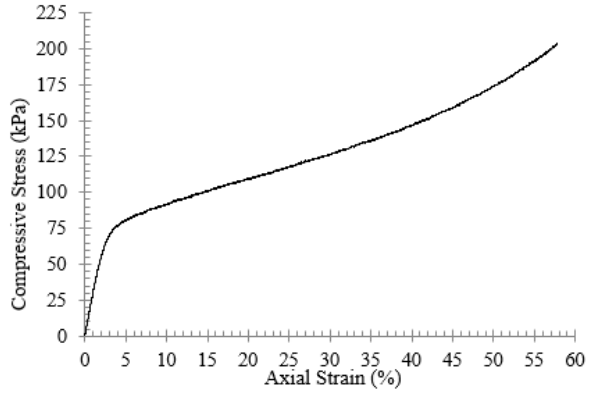

Fig. 1. Compressive stress versus axial strain relationship for EPS 20 geofoam material

2.2 Unconsolidated Undrained Triaxial Tests

To obtain the shear strength properties of EPS 20 geofoam, Unconsolidated Undrained Triaxial tests were carried out on cylindrical geofoam samples of height 76mm and diameter 38 mm (height to diameter ratio = 2). Tests were performed as per IS 2720 (Part 11):1993 with a constant displacemnt rate of 1.25 mm/min. Confining pressures of 50kPa, 100 kPa and 150 kPa were adopted. The results obtained are shown in the Figure 2.

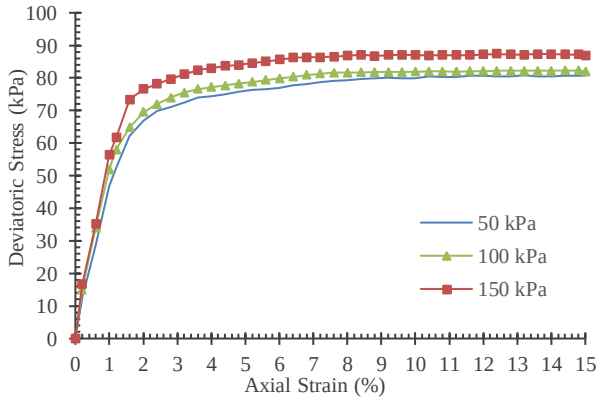

Fig.2. Unconsolidated Undrained Triaxial test results for EPS 20 geofoam

2.3 Modified Direct Shear Tests

According to Meguid and Khan (2019), the surface roughness of various interfaces plays a significant role in providing the shear resistance. To accurately obtain the shear parameters of various interfaces, modified direct shear tests were carried out for determining interface properties of geofoam-concrete, geofoam-sand, and sand-concrete interfaces. Modified direct shear test involves application of shear strain along the interface of two different materials. Two different materials were placed in two

different halves of the shearing box, such that the shearing plane coincides with the interface of these two materials.

ASTM D5321-17 was followed in performing the modified direct shear tests. Shear box of size 100 x 100 x 50 mm was used to avoid any possible boundary effect. Sets of three modified direct shear tests were performed at three different normal stress levels of 25, 50 and 75 kPa for each interface. These normal stresses were adopted so as to represent the field conditions to be investigated. M40 Concrete, EPS 20 geofoam and Indian Standard Grade II sand (backfill) were used as the testing materials. EPS geofoam and concrete samples were accurately cut into blocks of size 99.5 x 99.5 x 25 mm so as to perfectly fit into one half of shear box. According to ASTM D3080/D3080M – 11, the failure stress condition is defined as the maximum shear stress attained, or in the absence of a peak condition, the shear stress at 10 percent relative lateral displacement. Relative lateral displacement is the displacement between the top half and bottom half of the shear box.

A total of nine experiments were performed, three for each interface combination (geofoam-concrete, geofoam-sand, and sand-concrete). In all the experiments sand was placed at a relative density of 65% (15.93 kN/m$^{3)}$. In each interface shear test, harder material was placed in the bottom half of the direct shear box, so as to ensure that the shearing plane exactly coincides with the interface and also it prevents the tilting of shearing plane that may develop due to the differential settlement of geofoam. Dial gauges were used to take vertical and horizontal displacement measurements, proving ring was used to measure the shear force across the shear plane. The test is displacement controlled in nature and horizontal displacement was applied to the lower half of the shear box. A shearing rate of 1.25mm/min was adopted. No area correction was taken into account.

Table 1. Summary of interface shear test results

Test	Parameter	Value
Concrete - Geofoam	Adhesion (α) (kPa)	1
	ϕ (deg.)	30
Concrete - Sand	Adhesion (α) (kPa)	7
	ϕ (deg.)	32
Sand - Geofoam	Adhesion (α) (kPa)	10
	ϕ (deg.)	27

3. Calibration of numerical model and interface elements

The results obtained from the static compression tests were used to calibrate the Mohr-Coulomb constitutive law used in modelling of EPS geofoam material. Interface shear test results were used to calibrate the interface elements used in the numerical modelling. To calibrate the constitutive law used in modelling of EPS geofoam, static compression tests were numerically simulated and obtained stress-strain relation was compared with that of experimental result.

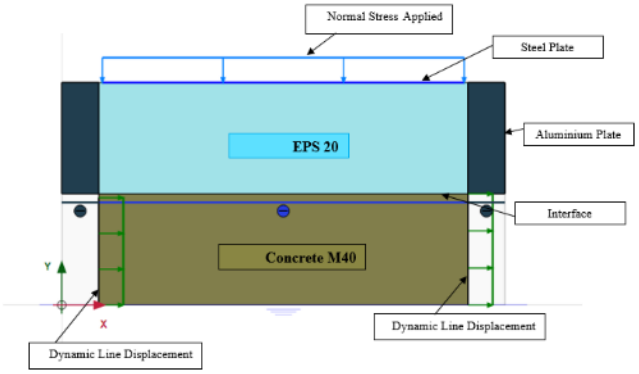

Fig.3. Plane strain numerical model of interface shear test

Table 2. Material parameters of various materials and interfaces

Material	Concrete	Sand	Sand -Concrete Interface	Sand -Geofoam Interface	Concrete -Geofoam Interface
Constitutive Model	Linear elastic	Mohr–Coulomb	Mohr–Coulomb	Mohr–Coulomb	Mohr–Coulomb
Unit weight, γ (kN/m^3)	25	15.93	15.93	15.93	0.2
Cohesion, c′ (kPa)	--	0	7	10	1
Friction angle, φ′ (deg.)	--	39	32	27	30
Initial Modulus, (kPa)	1.4 x 10^7	13000	13000	13000	3028
Poisson's ratio, ν	0.25	0.25	0.25	0.25	0.1
$R_{Interface}$	1	0.8	0.785	0.925	0.9

For calibration of interface elements interface shear tests were numerically simulated by varying $R_{Interface}$ value until the numerical predictions are matched with that of experimental results.

4. Development of Numerical model

4.1 Validation of Numerical Model

Ertugrul and Trandafir (2011) carried out small-scale physical model tests on rigid non-yielding wall models with and without EPS geofoam compressible inclusions. The results of these physical model tests were used to validate the numerical model used in the present study.

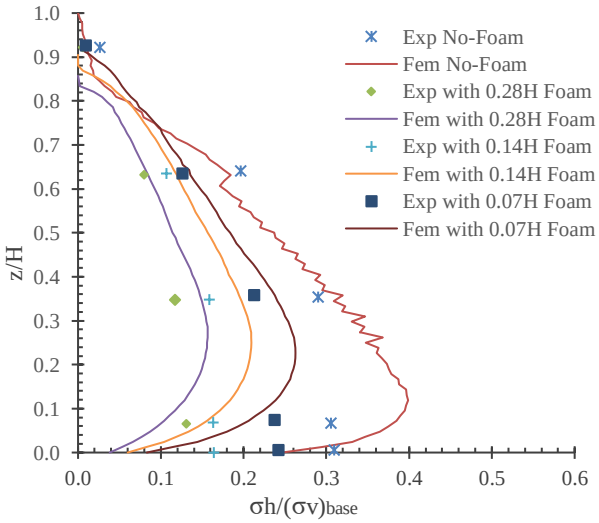

Fig.4. Comparison of results of numerical model used in current study with small-scale physical model test results by Ertugrul and Trandafir (2011)

Accurate predictions of lateral earth pressures were observed in top two-thirds portion of the wall giving confidence in the elastoplastic Mohr-Coulomb model that was adopted in the current study. Hence same constitutive law was used in predicting the lateral earth pressures on rigid retaining walls of field-scale.

4.2 Numerical Parametric Analysis

Numerical parametric study has been carried out to study the effect of wall height, inclusion thickness and inclusion density on the extent of lateral earth pressure reduction on the rigid retaining wall. The backfill material, foundation soil and EPS geofoam inclusion were modelled using the Mohr-Coulomb constitutive law. The parametric study has been carried out considering five different wall heights, four different geofoam densities and five different
geofoam inclusion thicknesses. The material parameters required for foundation material were taken from Ertugrul and Trandafir (2011). Indian Standard Grade II sand was used as backfill material. The properties of various materials used in numerical analysis are shown in Table 2 and Table 3. The list of various parameters considered in analysis were presented in Table 4. Boundary conditions of the numerical model were as shown in the figure 6. To simulate the on - field conditions, stage wise constriction is carried out in modelling the wall. The extent of foundation soil behind the wall is maintained at 3m in all the cases. The backfilling is done in six stages for all the wall heights.

The stage wise construction is carried out in the following manner.

Initial Phase: Normal ground condition (No loading).

Phase 1: Construction of retaining wall.

Phase 2: Placing of geofoam behind the retaining wall throughout the wall height.

Phase 3: Placing of first layer of the backfill material.
Phase 4: Placing of second layer of the backfill material.
Phase 5: Placing of third layer of the backfill material.
Phase 6: Placing of fourth layer of the backfill material.
Phase 7: Placing of fifth layer of the backfill material.
Phase 8: Placing of sixth layer of the backfill material.

Table 3. Mechanical properties of EPS geofoam inclusion material (Padade and Mandal, 2012)

Material	Density (kN/m^3)	Initial Modulus (kPa)	Cohesion (kPa)	Friction Angle φ (°)
EPS 15	0.15	2480.76	33.75	1.5
EPS 20	0.20	4070.55	38.75	2
EPS 22	0.22	5508.16	41.88	2
EPS 30	0.30	7550.28	62.00	2.5

Table 4. Variables used in the present study

Parameter	Value
Wall Height (H)	3m, 4.5m, 6m, 9m, 12m.
Geofoam Density	EPS 15, EPS 20, EPS 22, EPS 30
Inclusion Thickness (t)	0.05H, 0.10H, 0.15H, 0.20H, 0.25H

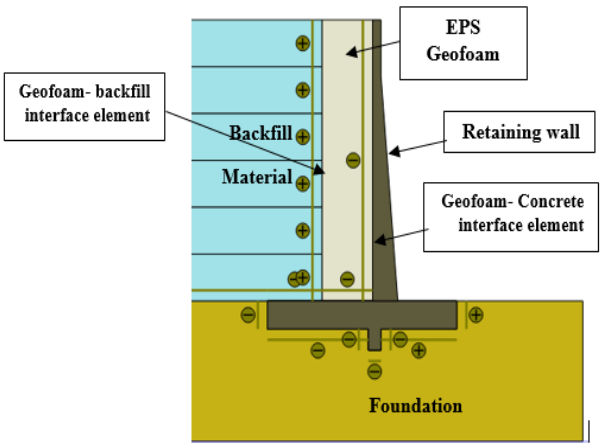

Fig.5. Detailed view of the 6m height retaining wall with 0.2H thick EPS 15 geofoam inclusion

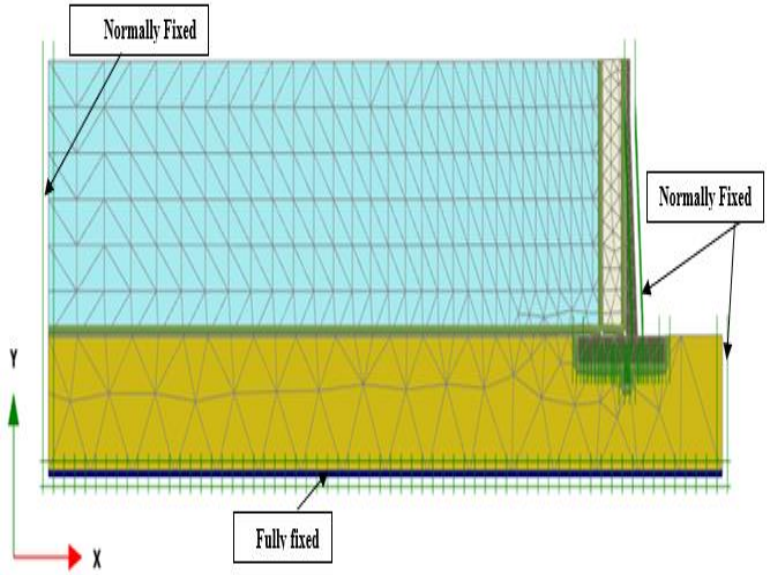

Fig.6. Deformed mesh of 6m height retaining wall with 0.20H thick EPS 15 geofoam inclusion

5. Results and Discussion

In total 100 (5 x 4 x 5) numerical simulations were carried out in the present parametric study. Five different wall heights (3m, 4.5m, 6m, 9m, and 12m), four different geofoam densities (EPS 15, EPS 20, EPS 22 and EPS 30) and five different geofoam inclusion thicknesses (0.05H, 0.10H, 0.15H, 0.20H and 0.25H) were considered. Total lateral earth force (per unit length), isolation efficiency and maximum lateral earth pressure were calculated for each case and were compared with that of standard control case (without inclusion) to evaluate the influence of various parameters. The total force per unit length (p_x) was calculated using

$$p_x = \int_0^H \sigma_x dz \qquad (1)$$

Isolation efficiency (i_p) was calculated using

$$i_p = \frac{p_o - p}{p_o} \text{ x } 100 \qquad (2)$$

Where p_o is lateral force per unit length on the wall without the inclusion and p is the lateral force per unit length on the wall with inclusion.

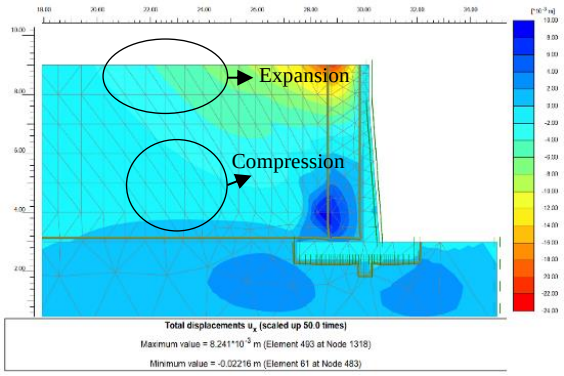

Fig.7. Total displacement profile of the retaining wall of height 6m with inclusion thickness of 0.20H

Considerable lateral movements were observed behind the retaining wall in its lower half-region due to the compression of geofoam inclusion resulting in the lateral movement of backfill material without any retaining wall movement. Even though the EPS geofoam is modelled as Elastoplastic material, the observed strains in majority of the cases in the current study were well within the elastic limit (1.5%) of the geofoam.

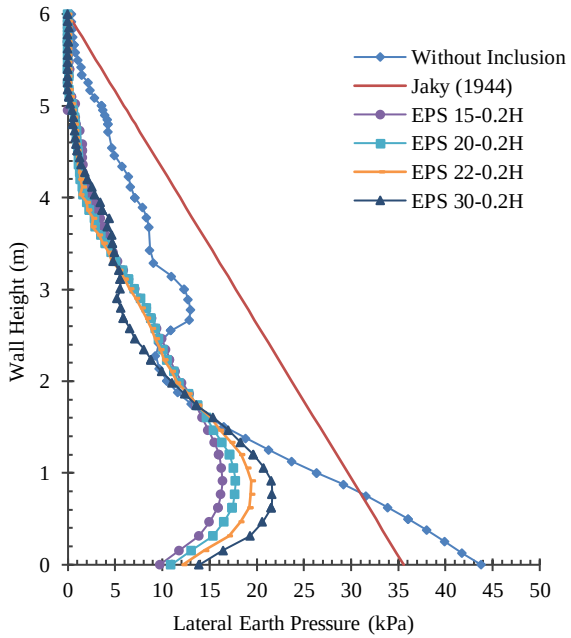

Fig.8. The variation of lateral earth pressure profile with EPS geofoam density for a 6m height retaining wall with 0.20H geofoam inclusion relative thickness

From the present analysis, among all the cases, highest isolation efficiency of 46.66% was observed for 6m height retaining wall with EPS 15 geofoam inclusion of 0.25H relative thickness. The isolation efficiency increased with increase in the wall height up to 6m, beyond which it decreased. The isolation efficiency was also found to increase with the increase in inclusion thickness and decrease with increase in geofoam density provided that the other parameters were kept constant.

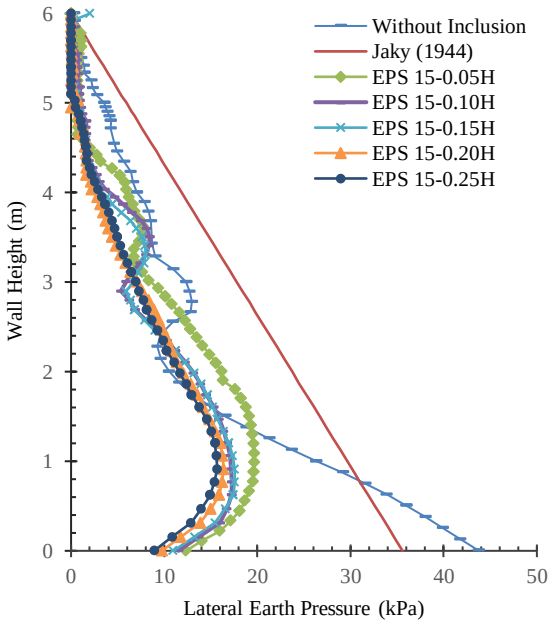

Fig.9. The variation of lateral earth pressure profile with EPS relative thickness for a 6m height retaining wall with EPS 15 geofoam inclusion

6. Conclusions

1. EPS geofoam density and its relative thickness play a predominant role in the extent of lateral earth pressure reduction.
2. From the calculated lateral displacements of backfill material, considerable magnitude of lateral displacements was observed in the lower-half of the retaining wall with compressible inclusion, thus allowing backfill soil to yield, resulting in the reduction of total lateral earth thrust on the wall.
3. It was noted that for a given relative thickness of geofoam inclusion, with the increase in EPS geofoam density, there is decreasing trend in the isolation efficiency of the compressible inclusion.
4. The isolation efficiency was observed to improve with the increase in the relative thickness of EPS inclusion for a given inclusion density.

5. The isolation efficiency improved with increase in the height of the retaining wall up to 6m height. Beyond 6m the isolation efficiency reduced with increase in the wall height.
6. Maximum isolation efficiency of 46.66% was observed for 6m height retaining wall with EPS 15 geofoam with relative inclusion thickness of 0.25H.

References

1. ASTM D5321: Standard test method for determining the coefficient of soil and geosynthetic or geosynthetic and geosynthetic friction by the direct shear method, American Society of Testing Materials, West Conshohocken (2017).
2. ASTM D1621: Standard Test Method for Compressive Properties of Rigid Cellular Plastics, West Conshohocken (2010).
3. ASTM D3080: Standard test method for direct shear test of soils under consolidated drained conditions, American Society of Testing Materials, West Conshohocken (2011).
4. ASTM D6817, Standard specification for rigid cellular polystyrene Geofoam. American Society of Testing Materials, West Conshohocken (2006).
5. Ertugrul, O.L. and Trandafir, A.C.: Reduction of lateral earth forces acting on rigid non-yielding retaining walls by EPS geofoam inclusions. Journal of Materials in Civil Engineering, 23(12), pp.1711-1718 (2011).
6. Gade, V.K.: Reduction of Earth Pressure on Rigid Non-Yielding Retaining Walls Subjected to Traffic Loading using EPS Geofoam. Doctoral dissertation. Indian Institute of Technology Bombay, Mumbai (2018).
7. Horvath, J.S.: Integral-abutment bridges: problems and innovative solutions using EPS geofoam and other geosynthetics. Research. Report. No. CE/GE-00-2, (2000).
8. Horvath, J.S.: An overview of the functions and applications of cellular geosynthetics. In: International e-Conference on Modern Trends in Foundation Engineering: Geotechnical Challenges and Solutions. https://www.ecfg.iitm.ac.in/, India (2003).
9. IS 2720-Part 11: Determination of the shear strength parameters of a specimen tested in unconsolidated undrained triaxial compression without the measurement of pore water pressure, Bureau of Indian Standards, New Delhi (1993).
10. IS 2720 -Part 13: Method of test for soils, direct shear test, Bureau of Indian Standards, New Delhi (1986)
11. Meguid, M.A. and Khan, M.I.: On the role of geofoam density on the interface shear behavior of composite geosystems. International Journal of Geo-Engineering 10(1), 6 (2019).
12. Padade, A.H. and Mandal, J.N.: Behavior of expanded polystyrene (EPS) geofoam under triaxial loading conditions. Electronic Journal of Geotechnical Engineering 17, 2542-2553 (2019).